Double-pulse electronic speckle interferometry for vibration analysis

Giancarlo Pedrini and Hans J. Tiziani

We describe a double-pulse electronic-speckle-interferometry system. Two separate speckle patterns of an object being tested are recorded within a few microseconds with a CCD camera. Their two images are stored in a frame grabber. The fringes obtained from subtraction are quantitatively analyzed by the spatial-carrier phase-shift method. Using three directions of illumination and one direction of observation, one can record at the same time all the information necessary for the reconstruction of the three-dimensional deformation vector. Applications of this system for measuring the rotating objects are discussed for the case for which a derotator needs to be used. Experimental results are presented.

1. Introduction

For measurement of vibrations by double-pulse techniques, pulse separations in the 1–1000-μs range are necessary. Until now double-pulse holographic interferometry has been used extensively in the study of vibrations.[1] A disadvantage of this method is that both the recording and the reconstruction of the vibration with a hologram are needed. For the recording a photographic plate or a thermoplastic camera is usually used. The hologram is usually reconstructed with a continuous laser and can be viewed with a CCD camera. This process is time-consuming.

Double-pulsed electronic speckle interferometry[2–5] (ESPI) enables us to obtain correlation fringes that correspond to displacement without recourse to any form of photographic processing and plate relocation. The systems described in Refs. 4 and 5 use the subtraction method. Two separate speckle patterns are recorded within a few microseconds with a CCD camera. The two images are then stored in a frame grabber, and the subtraction method is applied. The correlation fringes obtained are of good contrast.

The spatial-carrier phase-shift method[5–12] permits a quantitative analysis of the interference fringes. All the information necessary for reducing an interferogram to a phase map is recorded simultaneously. Therefore this method is well suited to use with double-pulse speckle interferometry. The application of this method to double-pulse speckle interferometry with a ruby laser is discussed in Ref. 5.

For precision measuring, all three components of the deformation vector are needed,[13–15] which is the case of the modal analysis where the measuring results must be correlated with the numerical calculations. The double-pulse ESPI system described in Ref. 5 determines only one vector component of the deformation along one sensitivity vector. This system can be extended for the determination of the three components of the deformation when three different illumination directions and three observing cameras are used. The extended system is described in Section 4.

The application fields for the measurements of rotating objects are usually different from those for stationary objects,[16] for example, automobile brakes, tires, or fans. In Section 5 a system for measuring rotating objects with double-pulse ESPI is described in which an optical derotator is used to compensate the rotation of the object optically.

2. Electronic Recording of Two Speckle Patterns of a Vibrating Object

An experimental setup for double-pulse ESPI is shown in Fig. 1. The beam from the ruby laser is split into the object and the reference beams. The object beam is enlarged by a diverging lens and illuminates the object (O). The object is imaged onto the CCD

The authors are with the Institut für Technische Optik, Universität Stuttgart, Pfaffenwaldring 9, D-70569 Stuttgart, Germany.

Received 31 August 1993; revised manuscript received 14 March 1994.

0003-6935/94/347857-07$06.00/0.

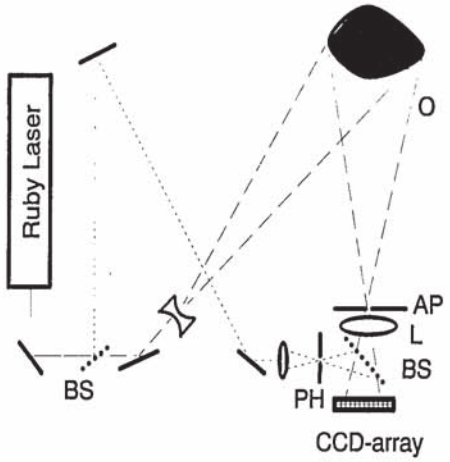

Fig. 1. Experimental setup for double-pulse ruby laser ESPI. BS, beam splitter; L, lens; PH, pinhole; AP, aperture.

camera by lens L. With the aperture (AP) in front of lens L it is possible to choose the optimal size of the speckle in the sensor plane. The interference pattern between the object and the reference beam is recorded by a CCD camera and changes with object vibration. We record the first image with the first pulse and the second image with the second pulse. The two images are then subtracted from each other, and the correlation fringes that correspond to the object deformation are obtained. For our experiments we used a ruby laser (wavelength, 694 nm) that can emit two high-energy pulses separated by a few microseconds. To record two images corresponding to the two pulses, an interline transfer CCD camera is used. This camera consists of an array of photosensors, each connected to a tap on a vertical shift register. Being illuminated, the photosensors generate charges that are transferred after a period of time into the shift register, which is covered to prevent the generation of new charges. The time necessary to transfer the charges from the photosensors to the shift register is short (2 or 3 μs, for example) because the transfer is parallel from each photosensor to the adjacent one. After the charge transfer the photosensors of the camera are ready for the new image. In our particular case we recorded the first pulse, and we transferred the charges to the shift register and then we recorded the second pulse. The two images (the first image in the shift register and the second image in the photosensors) can be read in two normal readout cycles, digitized, and stored into the frame memory. Because the two laser pulses usually do not have the same energy, a normalization of the two recorded speckle images is necessary. The absolute value of the subtraction of the two images is stored in the frame grabber. Figure 2 shows the subtraction between the two speckle patterns of a vibrating plate. The pulse separation was 100 μs. It was even possible to record two separate images with a pulse separation of 5 μs. Because the camera used in our experiment is interlaced, it is possible to transfer only the charges of the elements of the odd or even lines each time; therefore we use only half of the vertical resolution, but good results can still be obtained.

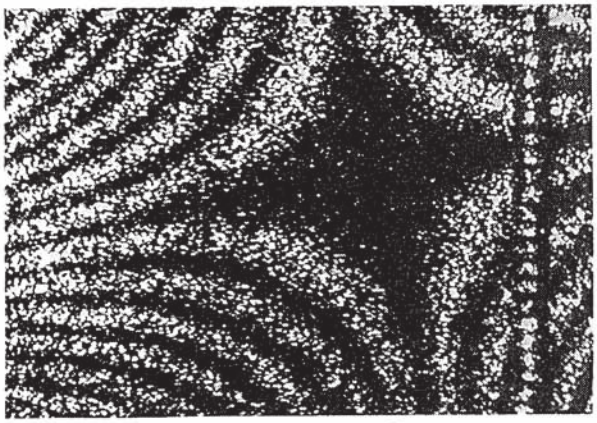

Fig. 2. Speckle interferogram of a vibrating plate recorded with a pulse separation of 100 μs.

3. Quantitative Analysis of the Fringes

A. Principle of the Fringe Analysis

The spatial-carrier phase-shifting method[5–12] is particularly well suited for use in a quantitative analysis of the fringes obtained from a pulsed laser, because all the information necessary to reduce an interferogram to a phase map can be recorded simultaneously. The reference beam is tilted by an angle θ with respect to the optical axis. In the image plane (where the CCD sensor is located) the speckle image of the object to be tested is then modulated with a carrier frequency with its period $p_M = \lambda/\sin\theta$. The angle θ is chosen so that the phase difference between the reference and object beams changes by a constant α from one pixel of the CCD camera to another. The first speckle pattern SP_1 of the object at position O_1 and the second SP_2 of the object at position O_2 are recorded and stored in the frame grabber. With the three-interferogram method speckle pattern SP_2 is shifted one pixel to the left (a digital shift in the frame grabber) with respect to SP_1; a subtraction between the two patterns is then performed, the square module is taken, and the image is averaged. Hence the intensity distribution I_1 is obtained by Eq. (1a). The second interferogram with an intensity distribution I_2 is obtained in the same way by Eq. (1b) without shifting one pixel. One obtains the third interferogram with intensity distribution I_3 by shifting one pixel to the right as in Eq. (1c):

$$I_1(x, y) = \langle |SP_1(x, y) - SP_2(x - \Delta x, y)| \rangle, \quad (1a)$$

$$I_2(x, y) = \langle |SP_1(x, y) - SP_2(x, y)| \rangle, \quad (1b)$$

$$I_3(x, y) = \langle |SP_1(x, y) - SP_2(x + \Delta x, y)| \rangle. \quad (1c)$$

The three intensities represent three phase-shifted fringe patterns, because the spatial carrier introduces a known constant phase shift (α) between successive pixels. The averaging $\langle\ \rangle$ eliminates the speckle noise; the sinusoidal fringes obtained can thus be

written in the following way:

$$I_1(x, y) = I_{01}(x, y)\{1 + b_1(x, y)\cos[\phi(x, y) - \alpha]\}, \quad (2a)$$

$$I_2(x, y) = I_{02}(x, y)\{1 + b_2(x, y)\cos[\phi(x, y)]\}, \quad (2b)$$

$$I_3(x, y) = I_{03}(x, y)\{1 + b_3(x, y)\cos[\phi(x, y) + \alpha]\}, \quad (2c)$$

where I_{0i} $(i = 1, 2, 3)$ are the average intensities, b_i are the modulation factors, α is the constant phase shift, and ϕ is the interference phase to be calculated. To apply this method it is necessary that the speckles are still correlated after the image shift of one pixel, which means that the pixel size should be greater than the period p_M. If this condition is satisfied, $I_{01} \cong I_{02} \cong I_{03}$ and $b_1 \cong b_2 \cong b_3$ are obtained. In this case Eqs. (2) become a system of three equations with three unknowns. Thus it is possible to calculate the phase ϕ at each point with the well-known relationship

$$\phi = \arctan\left(\frac{I_3 - I_1}{I_3 + I_1 - 2I_2}\tan\frac{\alpha}{2}\right), \quad (3)$$

where $\tan(\alpha/2)$ is unity if the phase shift is 90°.[9]

B. Experimental Results

We investigated the vibration of a plate a few microseconds after it was shocked by impact from a pendulum. To trigger the laser, an optical detector gave an electrical signal a few milliseconds before the pendulum hit the plate. This signal helps set the pulses of the ruby laser a few microseconds after the impact. The flash lamps are discharged to pump the ruby rod ~1 ms before the setting of the pulses. The metal pendulum and the metal plate are connected to the poles of battery; when the pendulum touches the plate the electrical circuit is closed. This produces an electrical impulse that is recorded on a memory oscilloscope, which permits one to know exactly when the impact takes place. The two laser pulses are recorded on another channel of the same oscilloscope. The two signals are then displayed to determine exactly the time interval between the impact and the pulses. Two interferograms are recorded with the two pulses and a tilted reference. After subtraction three phase-shifted images are obtained. The three images are then filtered with a 7 × 7 convolution low-pass filter and a 7 × 7 convolution median filter. The interferograms were evaluated by Eq. (3). Figure 3(a) shows the phase map of the deformation between 150 and 250 μs after the impact; the fringes seem to originate at the bottom right-hand corner of the figure, which was the point of excitation (the impact of the pendulum on the plate). We tried many times to repeat this experiment, and we always found the same deformation, which proves the reliability of our excitation system. We also repeated our experiment with the same excitation but by firing the two pulses at a different time. Figure 3(b) shows the deformation at 1 ms after the impact; the pulse separation was 100 μs as before. The deformation in Fig. 3(c) is clearly different from that in Fig. 3(a). Figure 3(c) shows the deformation at 2 ms after the impact (the pulse separation is still as before, 100 μs); a certain symmetry can be recognized. Figure 3(d) (with the same pulse separation of 100 μs) shows the

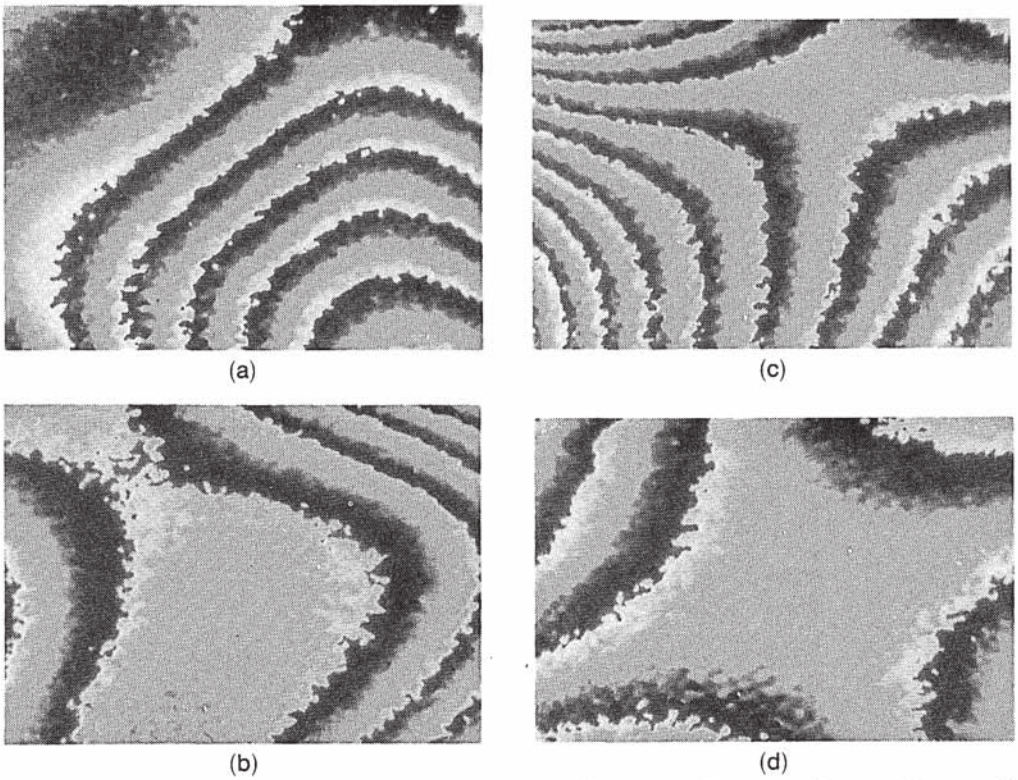

Fig. 3. Phase maps at different times after the impact of the pendulum on the plate: (a) 150 μs, (b) 1 ms, (c) 2 ms, (d) 1 s.

deformation at 1 s (a long time) after the impact. It is now possible to see that the vibration is harmonic.

4. Two- and Three-Dimensional Measurements

A. Principle of the Method

The results in Sections 2 and 3 are only one-dimensional, which means that they give the deformation of the object along only one sensitivity vector. The relationship between the phase $\phi(x, y)$ and the deformation is given by

$$\phi(x, y) = \frac{2\pi}{\lambda} \mathbf{u} \cdot \mathbf{s}, \tag{4}$$

where $\mathbf{u}$ is the desired displacement and $\mathbf{s}$ is the sensitivity vector that is given by the geometry of the setup:

$$\mathbf{s} = \hat{k}_i - \hat{k}_o, \tag{5}$$

where $\hat{k}_i$ and $\hat{k}_o$ are the unit vectors of illumination and observation, respectively.

In some cases a two-dimensional (2-D) or three-dimensional (3-D) analysis of the deformation is necessary. To determine the three components of the deformation vector it is necessary to measure the phase for three sensitivity vectors $\mathbf{s}_1$, $\mathbf{s}_2$, $\mathbf{s}_3$. (These sensitivity vectors should be noncoplanar.) The most convenient way to determine the deformation vector $\mathbf{u}$ is to decompose all vectors into their orthogonal components x, y, and z.[13] The orientation of the Cartesian system is arbitrary; for example, we can set the origin point on the object. If $\mathbf{s}_1 = (s_{1x}, s_{1y}, s_{1z})$, $\mathbf{s}_2 = (s_{2x}, s_{2y}, s_{2z})$, $\mathbf{s}_3 = (s_{3x}, s_{3y}, s_{3z})$, and $\mathbf{u} = (u_x, u_y, u_z)$, we can write the relationships among phases, sensitivity vectors, and deformation vectors in the matrix form:

$$\begin{pmatrix} \phi_1 \\ \phi_2 \\ \phi_3 \end{pmatrix} = \frac{2\pi}{\lambda} \begin{pmatrix} s_{1x} & s_{1y} & s_{1z} \\ s_{2x} & s_{2y} & s_{2z} \\ s_{3x} & s_{3y} & s_{3z} \end{pmatrix} \begin{pmatrix} u_x \\ u_y \\ u_z \end{pmatrix}. \tag{6}$$

This equation can be written in a more compact form:

$$\phi = \frac{2\pi}{\lambda} \mathscr{S} \cdot \mathbf{u}, \tag{7}$$

where $\mathscr{S}$ is called the sensitivity matrix. By knowing ϕ_1, ϕ_2, ϕ_3, and the sensitivity vectors $\mathbf{s}_1$, $\mathbf{s}_2$, and $\mathbf{s}_3$, we can determine the displacement vector $\mathbf{u}$ at each point of the object. In matrix form we obtain

$$\mathbf{u} = \frac{\lambda}{2\pi} \mathscr{S}^{-1} \cdot \phi, \tag{8}$$

where $\mathscr{S}^{-1}$ is the inverse of the sensitivity matrix. We can generate the sensitivity vectors by observing the object from different directions or by illuminating the object from different directions. One of the many methods[14] that generate the sensitivity vectors is to illuminate the object from one direction and observe it from three different directions with three different cameras. This method requires a simple setup, but its disadvantage is that it needs rectification because of the distortion by different observation directions. On the other hand, if three directions of illumination and one direction of observation are used, such a setup is more complicated than the last one but it has the advantage that it does not need rectifications. Therefore we chose this method for our investigation. Figure 4 shows the generation of two sensitivity vectors (for convenience) by the use of two directions of illumination and one direction of observation. The sensitivity vectors are given by the half-angle between illumination and observation directions [Eq. (5)]. Camera 1 records the interference between reference 1 (Ref. 1) and illumination 1 (ill. 1) and gives the phase map ϕ_1 that contains information about the deformation along the sensitivity vector $\mathbf{s}_1$. In the same way camera 2 gives phase map ϕ_2, which contains information about the deformation along vector $\mathbf{s}_2$. To avoid unwanted interference, the second reference/illumination beam pair is delayed. When a delay line is used, we have an additional incoherent speckle field caused by the object illumination. This field is the same for the two patterns recorded with the two laser pulses and disappears after subtraction of the speckle patterns. The incoherent speckle field reduces the number of bits available for the signal and produces a small reduction in the signal-to-noise ratio. The arrangement with three sensitivity vectors is based on the same principle, but it needs three illumination directions, three cameras, and two delay lines.

The measurement sensitivity is not the same for the three axes (x, y, z); the error for in-plane components (u_x, u_z) is larger than the error for out-of-plane components (u_y) because in practical cases the angle between the observation direction and the sensitivity vector must be smaller than 30°–40°.[14] If we assume

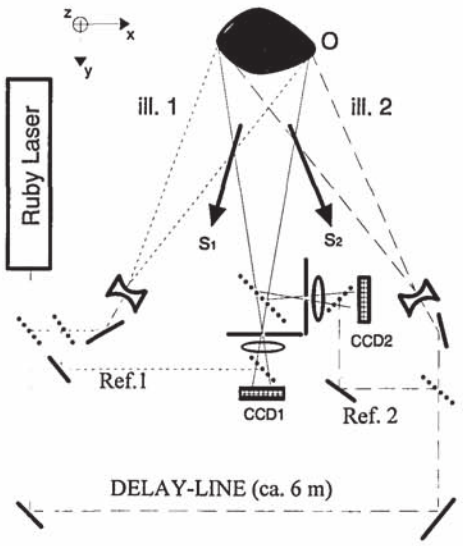

Fig. 4. Optical setup for 2-D speckle interferometry.

that the errors in the three phase measurements are equal and uncorrelated ($\delta\phi_x = \delta\phi_y = \delta\phi_z = \delta\phi$), the mean-square error of the displacement is

$$\langle \delta u_i^2 \rangle = \frac{\lambda^2 \delta\phi^2}{(2\pi)^2} \sum_k a_{ik}^2, \tag{9}$$

where $a_{ik} = \mathscr{S}^{-1}$ and $i, k = 1, 2, 3$.[15]

B. Experimental Results

With the setup in Fig. 4 where two sensitivity vectors are used, the projection of the deformation on the plane that contains the two sensitivity vectors can be determined. The second reference/illumination beam pair was delayed by 6 m with respect to the first, which corresponds to the coherence length of a pulse of a ruby laser that has a duration of 20 ns. The angles between the two illumination directions and observation direction were $-30°$ and $30°$, respectively; the two sensitivity vectors were in a horizontal plane. If the y axis is along the observation direction and the origin of the system is on the object, the two sensitivity vectors are $\mathbf{s}_1 = [\sin(-30°), 1 + \cos(-30°), 0] = (-0.5, 1{,}86, 0)$, $\mathbf{s}_2 = (\sin 30°, 1 + \cos 30°, 0) = (0.5, 1.86, 0)$. In Fig. 5 the object being tested was a cognac glass that was excited with a small pendulum. In this case we know from experience of measurements with other methods that the deformation occurs practically only in the horizontal plane (x, y) but not along the vertical axis z. This object is also well suited for analysis with a 2-D system. The two cameras are triggered together with the same external synchronization. Each camera is connected to its frame grabber located in a computer. (We thus had two cameras, two frame grabbers, and two computers.) Figures 5(a) and 5(b) show the two phase maps that we obtained by analyzing the fringes recorded with the two cameras. Note that in these phase maps we still have the 2π incertitude inside, which can be easily removed. In this example the bottom part of the glass in practice does not vibrate; the two phase maps were calibrated so that their 0 points concide with the 0 motion point of the object. From the phase maps it is then possible to calculate the deformation of the object projected on a horizontal plane. Using the 2-D case of Eq. (8) we calculate only u_x and u_y, because we had only two phase maps ϕ_1, ϕ_2. The relationship between the phase and the deformation in our configuration was $u_x = 2\pi/\lambda(\phi_1 - \phi_2)$ and $u_y = 0.26 \times 2\pi/\lambda(\phi_1 + \phi_2)$. Figure 5(c) shows the projection (on a horizontal plane) of the object deformation (u_x, u_y) along a line at the same height of the glass. For the representation of the deformation in two or three dimensions, the form of the object is needed. The form can be measured by different techniques, for example, a moiré or speckle interferometry technique.[17,18]

In Fig. 6 the object being tested was a vibrating plate where the surface was perpendicular to the observation direction. We chose this object because we know that the deformation in this case is perpendicular to the surface. By analyzing the fringes recorded by the two cameras, we can reconstruct the deformation along one line. Figure 6 confirms that this deformation is perpendicular to the surface, and our measurements are consistent. Unfortunately we did not have an object with the exactly known

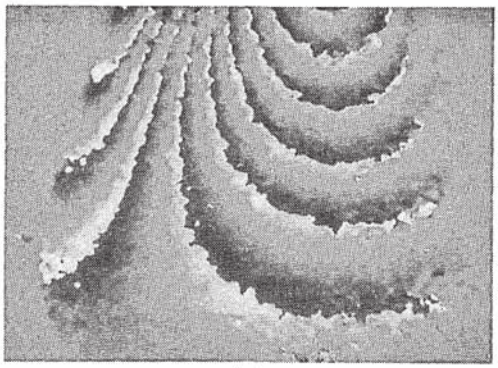

(a)

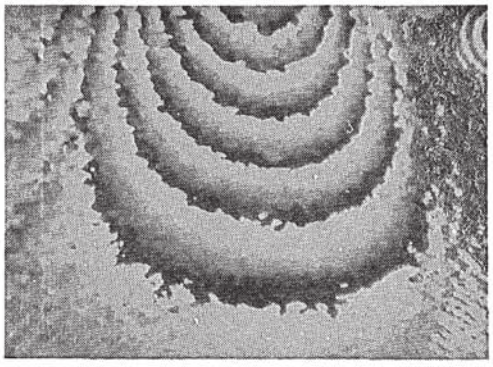

(b)

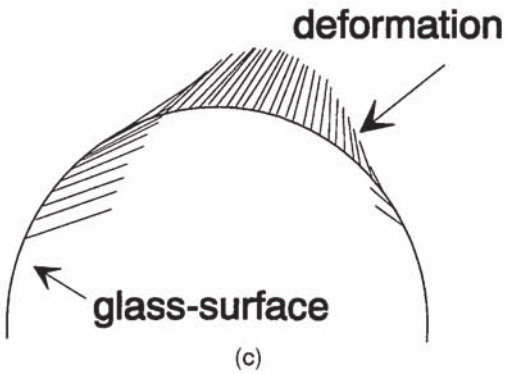

(c)

Fig. 5. Two-dimensional measurement of a cognac glass. (a) Phase map recorded with camera 1 leading to the deformation along the sensitivity vector $\mathbf{s}_1$. (b) Phase map recorded with camera 2 resulting in the deformation along the sensitivity vector $\mathbf{s}_2$. (c) Deformation along a line at the height h of the glass, obtained by combination of the deformations along the sensitivity vectors $\mathbf{s}_1$ and $\mathbf{s}_2$.

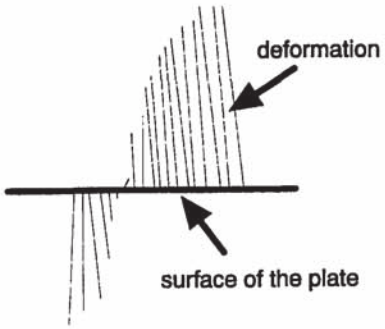

Fig. 6. Two-dimensional measurement of a vibrating plate: deformation along a horizontal line.

vibration data; it was also not possible to perform an accurate comparison or calibration measurement.

5. Double-Pulse ESPI for Vibration Measurement of Rotating Objects

It is difficult to measure the vibration of rotating objects because the objects rotate between the two exposures. To eliminate the object rotation, we used an image derotator. The image derotator[16] is a device by which the rotational motion of the object is compensated optically. A roof-edge prism rotating at half of the speed of the object produces a stationary image. For this purpose an angular encoder measures the rotation of the object; a derotator control unit drives a motor that rotates the prism. The arrangement is shown in Fig. 7. The axes of rotation of the object and derotator should be made collinear, and the observation and illumination directions should be made to coincide and be parallel to the rotation axis of the object and of the derotator. These two conditions are needed to obtain correlation fringes of good contrast that correspond to the out-of-plane (parallel to the rotation axis) deformation. To satisfy these conditions it is necessary to use beam splitter BS1 and BS2 in front of the rotating prism of the derotator to convey the derotated image to the CCD camera. Although a lot of the illumination is lost, on the other hand the alignment between illumination and observation directions is obtained. Lens L_2 images the object onto the CCD camera, and another beam spitter is used to introduce the reference wave as we see from Section 2.

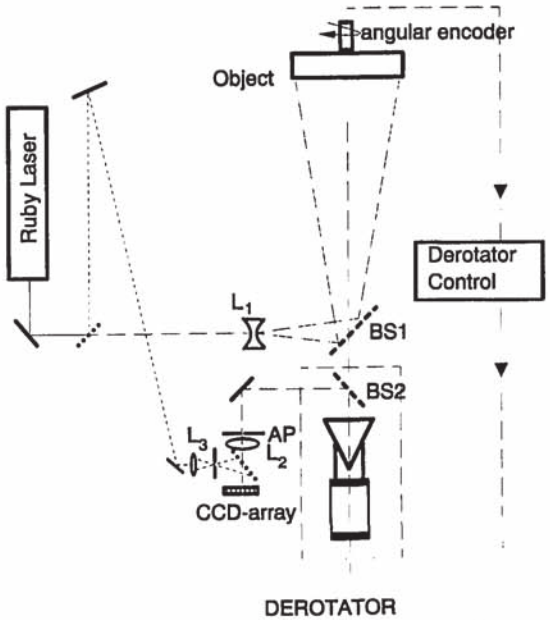

Fig. 7. Optical setup for double-pulse speckle interferometry with a rotating object.

For our experiment a thin plate (with a thickness of 0.5 mm) with a diameter of 12 cm was used; this plate was driven by a small electrical motor. To align the system, we adjusted first the two rotating axes (object and derotator axes) so that they are parallel. This task is easily accomplished by illuminating the object (for example, with white light not collinear to the axis of rotation) and by adjusting the derotator until a stable image of the object is observed (which can be observed, for example, by a CCD camera). For the virtual point source of divergence to be on the rotation axis, we must illuminate the rotating object with a He–Ne laser that is collinear with the ruby laser. At the output of the derotator we can observe the illuminated object. The direction and the virtual diverging point of the illumination beam are adjusted until a stable speckle pattern is obtained, which means that the derotator compensates the in-plane rotation of the object and the virtual point of the illumination source lies on the rotation axis.

Figure 8(a) shows a phase map obtained with this arrangement and the object points out. In this case

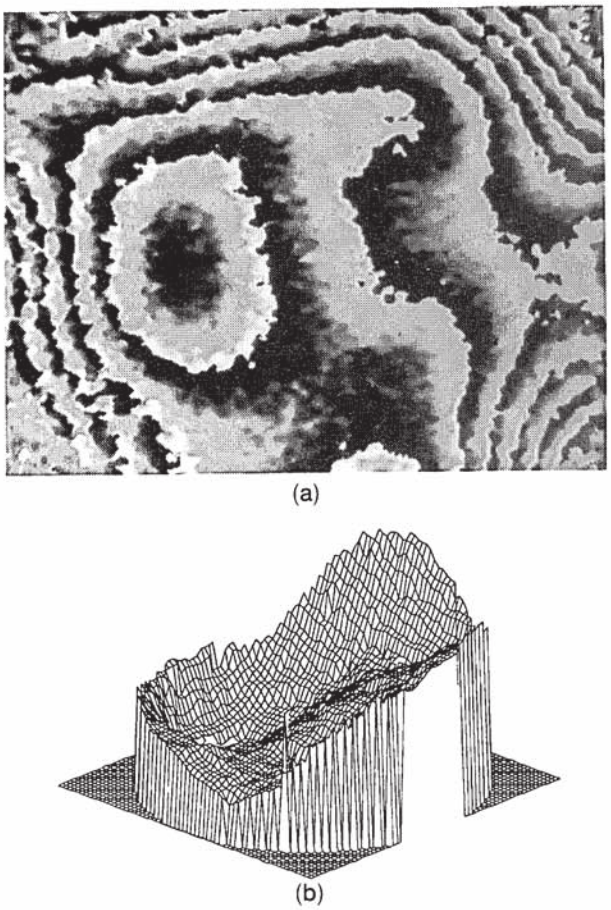

Fig. 8. Double-pulse speckle interferometry with a plate rotating at 3000 rpm and a pulse separation of 200 μs: (a) phase map, (b) pseudo-3-D representation of the deformation.

the frequency of rotation was 3000 rpm and the pulse separation 200 μs. We could observe that the contrast in the fringes after the subtraction was worse than in the case in which the objects were not rotated, probably because our illumination beam was not uniform, and thus a certain part of the object (since it rotates) is illuminated differently between the two exposures. Hence the speckle correlation decreases and the fringe contrast after subtraction is poor. For this reason the phase map contains quite a lot of noise, but an analysis is still possible as shown in Fig. 8(b) with a pseudo 3-D representation of the deformation. The phase map does not contain straight fringes that are generated from in-plane rotations, which means that the system is quite well aligned and only the out-of-plane deformations are obtained.

6. Conclusions

The double-pulse speckle interferometry method described in this paper is a powerful tool for the analysis of vibrations. In particular, the pulse separation in the range of 0.01–1 ms permits the study of transient events.

The double-pulse speckle interferometry method is much simpler than the double-pulse holographic interferometry and permits a quick analysis of the interferograms without the development of films and hologram reconstructions. Thus it is well suited to industrial applications. Currently the quantitative analysis is not as accurate as in the case of holographic interferometry. In fact the speckle size during our experiments was quite large (40 μm) because the CCD camera used in the experiment has pixel cells with sizes of 11×11 μm^2. One can improve the accuracy by using cameras with more pixels of smaller size, which will certainly be available in the near future.

One can certainly extend the system to determine the three components of the deformation by illuminating the object from three directions and by observing with three cameras. Three-dimensional measurements are necessary for a modal analysis in which the results must be correlated with the numerical calculations. A system by which two components of the deformation were measured was tested in our laboratory.

Double-pulse ESPI can be used to measure rotating objects with an optical derotator that compensates the rotation of the object optically. Note that during the experiments reported above the ruby laser was operated close to its threshold. (In fact the objects were quite small.) By operating the ruby laser at higher energy, one can record interferograms of larger objects, e.g., 1×1 m^2.

The authors thank Y. L. Zou for many helpful discussions and the German Federal Ministry for Research and Technology for financial support.

References

1. W. Sixt and J. Engelsberger, "Holographic applications of computer-based fringe interpretation," in *Optics in Engineering Measurement,* W. F. Fagan, ed., Proc. Soc. Photo-Opt. Instrum. Eng. **599,** 97–104 (1985).
2. T. J. Cookson, J. N. Butters, and H. C. Pollard, "Pulsed laser in E.S.P.I.," Opt. Laser Technol. **10,** 119–124 (1978).
3. J. R. Tyrer, "Application of pulsed holography and double pulsed electronic speckle pattern interferometry to large vibrating engineering structures," in *Optics in Engineering Measurement,* W. F. Fagan, ed., Proc. Soc. Photo-Opt. Instrum. Eng. **599,** 181–185 (1985).
4. R. Spooren, "Double-pulse subtraction TV holography," Opt. Eng. **31,** 1000–1007 (1992).
5. G. Pedrini, B. Pfister, and H. J. Tiziani, "Double pulse-electronic speckle interferometry," J. Mod. Opt. **40,** 89–96 (1993).
6. M. Kujawinska and J. Wojciak, "Spatial phase shifting techniques of fringe pattern analysis in photomechanics," in *Moiré Techniques, Holographic Interferometry, Optical NDT, and Applications to Fluid Mechanics,* F. Chiang, ed., Proc. Soc. Photo-Opt. Instrum. Eng. **1554B,** 503–513 (1991).
7. M. Küchel, "The new Zeiss interferometer," in *Optical Testing and Metrology III: Recent Advances in Industrial Optical Inspection,* C. Grover, ed., Proc. Soc. Photo-Opt. Instrum. Eng. **1332,** 655–663 (1990).
8. B. Pfister, M. Beck, and H. J. Tiziani, "Speckleinterferometrie mit alternativen Phasenshiebe- methode an Beispielen aus der Defektanalyse," in *Laser in der Technik: Vorträge des 10. Internationalen Kongresses Laser 91,* W. Waiderlich, ed. (Springer-Verlag, Berlin, 1992), pp. 63–67.
9. B. Pfister, "Speckleinterferometrie zur Defektanalyse mit neuen Phasenschiebenmethoden," Ph.D. dissertation (Universität Stuttgart, Stuttgart, Germany, 1993).
10. S. Leidenbach, "Die direkte Phasenmessung-ein neues Verfahren zur Berechnung von Phasenbildern aus nur einem Intensitätsbild," in *Laser in der Technik: Vorträge des 10. Internationalen Kongresses Laser 91,* W. Waiderlich, ed. (Springer-Verlag, Berlin, 1992), pp. 68–72.
11. H. Steinbichler, "New options of holographic metrology," in *Holographic Optics III: Principles and Applications,* G. M. Morris, ed., Proc. Soc. Photo-Opt. Instrum. Eng. **1507,** 435–447 (1991).
12. D. C. Williams, N. S. Nassar, J. E. Banyard, and M. S. Virdiee, "Digital phase-step interferometry: a simplified approach," Opt. Laser Technol. **23,** 147–150 (1991).
13. C. M. Vest, *Holographic Interferometry* (Wiley, New York, 1979), Chap. 2, p. 75.
14. A. Ettemeyer, "Statische Verformungen," in *Praxis der Holografie: Grundlagen Standard- und Spezialverfahren,* H. Marwitz, ed. (Expert Verlag, Ehningen bei Böblingen, 1990), pp. 224–244.
15. R. Thalmann, "Electronic fringe interpolation in holographic interferometry," Ph.D. dissertation (University of Neuchatel, Neuchatel, Switzerland, 1986).
16. M.-A. Beeck, "Pulsed holographic vibration analysis on high-speed rotating objects: fringe formation, recording techniques, and practical applications," Opt. Eng. **31,** 553–561 (1992).
17. C. Joenathan, B. Pfister, and H. J. Tiziani, "Contouring by electronic speckle pattern interferometry," Appl. Opt. **29,** 1905–1911 (1990).
18. X. Peng, H. Y. Diao, Y. I. Zou, and H. J. Tiziani, "Contouring by modified dual-beam ESPI based on tilting illumination beams," Optik **2,** 61–64 (1992).